

## Preparation and Physical Properties of (La, Pr)BaMnMoO<sub>6</sub> Double Perovskite Series

Meaz<sup>1\*</sup>T.M., S. Tajima<sup>2</sup>, S. A. Saafan<sup>1</sup>, S. Miyasaka<sup>2</sup>, M. K. El Nimir<sup>1</sup>, and R. E. El Shater<sup>1&2</sup>

<sup>1</sup> Physics Department, Faculty of Science, Tanta University, 31527 Tanta, Egypt.

<sup>2</sup> Department of Physics, Graduate School of Science, Osaka University, Osaka 560-0043, Japan.

[tmeaz@yahoo.com](mailto:tmeaz@yahoo.com)

[tmeaz@science.tanta.edu.eg](mailto:tmeaz@science.tanta.edu.eg)

**Abstract:** A series of La<sub>1-x</sub>Pr<sub>x</sub>BaMnMoO<sub>6</sub> double perovskite has been prepared, and their physical properties have been investigated. Polycrystalline samples of this system with x=0 – 1.0 could be synthesized at high temperature of 1623 K in the flowing of Ar+H<sub>2</sub> forming gas with relatively high H<sub>2</sub> concentration of 7 %. The results of powder X-ray diffraction and the Rietveld analysis indicate that the crystal structure of the La<sub>1-x</sub>Pr<sub>x</sub>BaMnMoO<sub>6</sub> series is cubic with space group of *Fm3m*. The lattice parameters and bond lengths of La/Pr/Ba-O and Mn/Mo-O have been estimated too, and they have been found to reduce with Pr doping. The decrease of bond length by Pr doping enhances the nearest-neighbor interaction between Mn<sup>2+</sup> and Mo<sup>5+</sup> spins, and increases the ferrimagnetic transition temperature, which has been observed in the temperature-dependent susceptibility. The shrinkage of crystal structure by the substitution of Pr increases not only the nearest-neighbor interaction but also the next-nearest-neighbor ones between spins on Mn<sup>2+</sup> sites or on Mo<sup>5+</sup> ones. In addition, the results of magnetic-field-dependent magnetic moment indicate that the Pr doping enhances the ferromagnetic interactions, and changes the behavior of low-temperature susceptibility from spin-glass like behavior to cluster-glass one. The reduction of bond length by Pr doping also increases carrier hopping, and reduces the magnitude of resistivity. Moreover, all the samples show semiconducting behavior which is well explained by the variable range hopping model in the whole temperature range.

[Meaz T.M., S. Tajima, S. A. Saafan, S. Miyasaka, M. K. El Nimir and R. E. El Shater. **Preparation and Physical Properties of (La, Pr)BaMnMoO<sub>6</sub> Double Perovskite Series.** *J Am Sci* 2012;8(7):844-852]. (ISSN: 1545-1003). <http://www.jofamericansscience.org>. 123

**Keywords:** Double Perovskites; Magnetic Susceptibility; Magnetic Moment; Resistivity.

### 1. Introduction

A variety of oxides showing interesting magnetic properties belong to the perovskite structure. The rare-earth based manganates are perhaps the most widely studied among the perovskite-based magnetic oxides. These oxides can exhibit a range of properties and shot into prominence with the discovery of colossal magnetoresistance [1]. The perovskite-type oxides have a general formula of ABO<sub>3</sub>, in which A and B represents an alkaline-earth (or rare-earth) cation and a transition-metal one, respectively. The cubic perovskite structure is constructed by corner-shared BO<sub>6</sub> octahedra and A cations at 12-coordinate sites. One of perovskite-related compounds, double perovskite-type oxides have attracted a broad interest, because of their unique structure, complicated magnetism, large magnetoresistance around room temperature. [2-4] Double perovskite-type oxides have the formula A<sub>2</sub>BB'O<sub>6</sub>, where the prime indicates the different ions with different valence numbers. The transition-metal cations of B and B' are regularly ordered, i.e. the alternate arrangement of B and B' ions have been observed over the six-coordinate B/ B' sites. Since the transition-metal ions in the perovskite-related compounds generally determine the electronic and magnetic structures, the alternating order of the

different kinds of B and B' ions are expected to cause a variety of the physical properties of double perovskite oxides. One of the famous compounds is, Sr<sub>2</sub>FeMoO<sub>6</sub> in which Fe<sup>3+</sup> (spin quantum number S=5/2) and Mo<sup>5+</sup> (S=1/2) ions order alternatively on the B-sites and the respective spins couple antiferromagnetically [4].

A<sub>2</sub>MnMoO<sub>6</sub> (A=Ca, Sr, Ba) contains Mn<sup>2+</sup> with magnetic moment of 5 μ<sub>B</sub> and Mo<sup>6+</sup> with no magnetic moment leading to the next-nearest-neighbor superexchange (antiferromagnetic) interaction. In contrast with the ferromagnetic behaviors in Sr<sub>2</sub>FeMoO<sub>6</sub>, A<sub>2</sub>MnMoO<sub>6</sub> consequently undergo the magnetic order to antiferromagnetic state at low temperatures [5-7]. Many researchers introduced La<sup>3+</sup> (4f<sup>0</sup>, 0 μ<sub>B</sub>) ion to the A site in the A<sub>2</sub>MnMoO<sub>6</sub> to produce LaAMnMoO<sub>6</sub> [8-12]. This doping changed the magnetic property of the mother compounds. Introducing La<sup>3+</sup> changed the cation valence of Mo<sup>6+</sup>(4d<sup>0</sup>, 0 μ<sub>B</sub>) to Mo<sup>5+</sup>(4d<sup>1</sup>, 1 μ<sub>B</sub>) and caused the nearest-neighbor superexchange interaction between the spins of Mn<sup>2+</sup> and Mo<sup>5+</sup>. As a result, LaAMnMoO<sub>6</sub> show ferrimagnetism with various Curie temperatures depending on the cation of A and the preparation conditions.

In the present work, the double perovskite-type systems with B/ B'=Mn/Mo have been investigated.

And since introducing  $\text{La}^{3+}$ , which has no net magnetic moment, changed the magnetic behavior of  $\text{A}_2\text{MnMoO}_6$  compounds, the substitution of other lanthanide cation ( $\text{Ln}^{3+}$ ) with a net magnetic moment to  $\text{LaAMnMoO}_6$  may give interesting results. The aim of this work is to study the effect of substitution of  $\text{Pr}^{3+}$  ( $4f^2$ ,  $4 \mu_B$ ) for  $\text{La}^{3+}$  in  $\text{LaBaMnMoO}_6$  compound on the structure and the physical properties.

## 2. Experimental

Polycrystalline series of  $\text{La}_{1-x}\text{Pr}_x\text{BaMnMoO}_6$  with  $x=0-1.0$  have been prepared by a conventional technique of solid state reaction. Starting materials of  $\text{BaCO}_3$  (High Purity Chemical Co., 99.95%),  $\text{La}_2\text{O}_3$  (High Purity Chemical Co., 99.99%),  $\text{Pr}_6\text{O}_{11}$  (rare metallic company LTD., 99.99%),  $\text{Mn}_3\text{O}_4$  (High Purity Chemical Co., 99.9%), and  $\text{MoO}_3$  (High Purity Chemical Co., 99.9%) have been thoroughly mixed and pressed into pellets. The pellets have been sintered in a tube furnace at 773K, 1173K, and 1623K in the flow of forming gas of  $\text{Ar}/\text{H}_2$  (93%/7%) and have been ground between the three sintering processes. In the final step the pellets have been cooled down to 1173K with a rate of 1 K/min and then to room temperature with a rate of 100 K/h. This cooling step is important to obtain a minimum spin disorder inside the materials. The high sintering temperature (1623K), and the high  $\text{H}_2$  concentration in the flowing gas have been used to overcome the impurity phase  $\text{Ln}_{1.4}\text{Mo}_{2.8}\text{O}_7$ , which had appeared with introducing high concentration of Pr at lower sintering temperatures below 1523K and/or in the flow of gas with lower  $\text{H}_2$  ratio below 5% in the first trials of preparation.

X-ray diffraction (XRD) measurements and Rietveld analysis have been performed by using an XRD diffractometer ( $\text{Cu K}_\alpha$  radiation) and FULLPROF program. Magnetic susceptibility measurements have been performed under both zero-field cooled (ZFC) and field cooled (FC) conditions with a SQUID magnetometer (Quantum Design, MPMS-7). The resistivity measurements have been performed by a four probe method down to 150 K.

## 3 Results and Discussion

### 3.1 Structural characteristics

The XRD profiles at room temperature reveals high purity phase of  $\text{La}_{1-x}\text{Pr}_x\text{BaMnMoO}_6$  compounds with various concentrations (x) of Pr. The unit cell parameters of the samples have been calculated by full profile fitting (FULLPROF program). Figure 1 shows the XRD profiles and the results of fitting for the  $x = 0.0$  and  $1.0$  samples only. The crystal structure of all  $\text{La}_{1-x}\text{Pr}_x\text{BaMnMoO}_6$  samples have given good fit to the cubic structure with space group  $Fm\bar{3}m$  in consistency with earlier reports [8-13]. For the

sample ( $\text{LaBaMnMoO}_6$  ( $x = 0.0$ )), the lattice constant is  $8.1184 \text{ \AA}$  which is in good agreement with previously published values of  $a = 8.1269 \text{ \AA}$  [8],  $8.1192 \text{ \AA}$  [9], and  $8.1174 \text{ \AA}$  [13]. The atomic positions of the two displayed samples:  $\text{LaBaMnMoO}_6$  ( $x = 0$ ) and  $\text{PrBaMnMoO}_6$  ( $x = 1.0$ ) are shown in table 1.

**Table 1:** Atomic positions of  $\text{La}_{1-x}\text{Pr}_x\text{BaMnMoO}_6$  ( $x=0$  and  $1.0$ ) at room temperature. For  $\text{LaBaMnMoO}_6$  ( $x=0$ ),  $a=8.118 \text{ \AA}$ ; space group:  $Fm\bar{3}m$ ;  $R_{wp}=16.89 \%$ ;  $R_p=10.57\%$ ;  $R_B=5.23\%$ . For  $\text{PrBaMnMoO}_6$  ( $x=1.0$ ),  $a=8.097 \text{ \AA}$ ; space group:  $Fm\bar{3}m$ ;  $R_{wp}=15.69 \%$ ;  $R_p=10.43\%$ ;  $R_B=4.62\%$ .

Atom	position	X	y	Z
Ba/La/Pr	8c	<b>0.25</b>	<b>0.25</b>	<b>0.25</b>
Mn	4a	<b>0.0</b>	<b>0.0</b>	<b>0.0</b>
Mo	4b	<b>0.5</b>	<b>0.5</b>	<b>0.5</b>
O ( $x=0$ )	24e	<b>0.2511(6)</b>	<b>0.0</b>	<b>0.0</b>
O ( $x=1.0$ )	24e	<b>0.2500(9)</b>	<b>0.0</b>	<b>0.0</b>

Figure 2(a), (b) and (c) shows the Pr content (x) dependence of lattice parameter ( $a$ ), tolerance factor ( $\tau$ ), and bond length ( $d_{\text{Mn/Mo-O}}$ ), respectively. The lattice parameter ( $a$ ) decreases as the Pr content (x) is increased. This decrease is due to the replacement of  $\text{La}^{3+}$  ions by smaller ions of  $\text{Pr}^{3+}$ . The tolerance factor in Figure 2(b) was calculated by using the obtained bond lengths of  $d_{\text{La/Pr/Ba-O}}$  and  $d_{\text{Mn/Mo-O}}$  as in equation (1).

$$\tau = d_{\text{La/Pr/Ba-O}} / (\sqrt{2} \langle d_{\text{Mn/Mo-O}} \rangle) \quad (1) [14]$$

$$\langle d_{\text{Mn/Mo-O}} \rangle = (d_{\text{Mn-O}} + d_{\text{Mo-O}}) / 2$$

The experimental results indicate a decrease of  $\tau$  with increasing Pr doping. Additionally, the x dependence of bond length of  $d_{\text{Mn/Mo-O}}$  in Figure 2(c) shows a small variation in lower doping region of  $x < 0.6$ , while it shows a greater decrease above  $x = 0.6$ . It will be seen in the next section that this decrease of the Mn-Mo distances strengthens the magnetic interaction.

### 3.2 Magnetic behavior

Figure 3 displays the temperature dependence of the *dc* magnetic susceptibility ( $\chi$ ) of the samples with  $x=0$ ,  $0.5$  and  $1.0$ . With decreasing temperature,  $\text{La}_{1-x}\text{Pr}_x\text{BaMnMoO}_6$  undergoes a ferrimagnetic transition around  $T_c=110-140 \text{ K}$ , (will be described later). As temperature is further lowered, the magnetic susceptibility is gradually enhanced, and shows spin glass or cluster glass below 50 K. For the  $x=0.0$  and  $0.5$  samples, the magnetic susceptibility has cusp around 25 K in both of ZFC and FC procedures in the low magnetic fields. In these compounds, the shapes of low-temperature magnetic susceptibility are dependent on the applied magnetic field. These behaviors are similar to the typical spin glass one

reported previously [8, 12, and 15]. As shown in Figure 3, the characteristic temperature of spin glass,  $T_G$ , is determined as the temperature at maximum point of the cusp of the magnetic susceptibility in the magnetic field of 0.01 T.

In  $\text{La}_{1-x}\text{Pr}_x\text{BaMnMoO}_6$ , the nearest-neighbor superexchange (antiferromagnetic coupling) interaction between  $\text{Mn}^{2+}$  and  $\text{Mo}^{5+}$  is dominant with ferrimagnetic property. In this system, however, the next-nearest-neighbor magnetic interaction of 180° or 90° bonds of  $\text{Mn}^{2+}$ -O-Mo-O-Mn<sup>2+</sup> cannot be ignored, and resultantly causes the suppression of the  $\text{Mn}^{2+}$ - $\text{Mo}^{5+}$  antiferromagnetic coupling [12]. The competition between the nearest-neighbor interaction and the next-nearest-neighbor one perhaps induces the magnetic frustration and the above-mentioned spin glass behavior in  $\text{La}_{1-x}\text{Pr}_x\text{BaMnMoO}_6$ .

As shown in Figure 3, the magnetic susceptibility for  $x=1.0$  in the ZFC measurement in low magnetic field has a broad peak around 40 K, while that in the FC procedure does not show the cusp or peak structure and monotonically increases with decreasing temperature. This behavior of magnetic susceptibility of the  $x=1.0$  sample is not qualitatively different from those of the  $x=0$  and 0.5. The shape of magnetic susceptibility for  $x=1.0$  shown in Figure 3 depends on the applied magnetic field. The difference between the ZFC and FC results almost disappears by applying magnetic field of 1.0 T. In smaller applied field, when the ZFC curve has a broad peak, the FC curve shows monotonous increase as temperature is lowered indicating the existence of cluster spin glass rather than the simple spin glass in  $x=1.0$  [15-18]. At low field, the divergence between the zero-field-cooled (ZFC) and field-cooled (FC) data indicates the presence of a weak ferromagnetic moment which can be ascribed to moment canting on the sublattices [17].

The present results indicate that the Pr substitution in this system induces the crossover from spin glass to cluster glass states above  $x=0.5$  at low temperatures, i. e. with increasing Pr content. Similar phenomena had been observed in the perovskite-type cobalt and manganese oxides [17, 19 and 20]. The Pr doping to rare-earth sites causes the decrease of bond length between  $\text{Mn}^{2+}$  and  $\text{Mo}^{5+}$ , and resultantly enhances both of nearest-neighbor and next-nearest-neighbor magnetic interaction. As described later, the Pr substitution for La clearly increases the ferromagnetic interaction in the investigated  $\text{La}_{1-x}\text{Pr}_x\text{BaMnMoO}_6$ . The large magnetic 4f moments of  $\text{Pr}^{3+}$  may enhance the ferromagnetic correlation in this system. These present results suggest that the enhancement of magnetic interaction, particularly ferromagnetic one, induces the magnetic

cluster and the crossover from spin glass to cluster glass states with introducing Pr to rare-earth sites.

There is a characteristic temperature  $T_C$  of ferrimagnetic transition, which can be estimated from the temperature dependence of the inverse of susceptibility as shown in Figure 4. As Pr is substituted to La sites,  $T_C$  is enhanced, indicating the increase of magnetic interaction. A linear temperature dependence of the inverse susceptibility is observed above  $T_C$ .

Figure 5 (a, b and c) display the magnetic-field-dependence of magnetic moment at various temperatures for the samples with  $x=0$ , 0.5 and 1.0, respectively. As is expected, the magnetic moment decreases with increasing temperature, and shows non-linear dependence of the applied magnetic field at low temperatures, but linear-dependence at high temperatures. In the  $x=1.0$  sample, the nonlinearity is observed below around  $T_C$ , suggesting the enhancement of ferromagnetic interaction and magnetic clusters.

Figure 6 shows the magnetic moment against applied field at 5K for all samples. The magnetic moment per formula does not saturate even with applied field up to 7T. It increases systematically as Pr is substituted to the system especially above  $x=0.5$ . In addition, there are some observed residual magnetic moment and hysteresis (magnification of two of the curves is displayed in the inset to clarify this hysteresis), these results agree with the above suggestion that the Pr doping increases the ferromagnetic interaction, and give greater weight to a suggestion that there is no superparamagnetism in this system [17].

Figure 7 represents the Pr concentration ( $x$ ) dependence of the effective magnetic moments ( $\mu_{\text{eff}}$ ), the magnetic moments at 5 K in magnetic field of 7 T ( $\mu_m$ ), the ferrimagnetic transition temperature ( $T_C$ ), and spin/cluster glass temperature ( $T_G$ ). The effective magnetic moment ( $\mu_{\text{eff}}$ ) and Weiss temperature ( $\theta$ ) can be estimated using simple Curie Weiss formula (equation (2)).

$$\chi = C/(T - \theta) \quad (2)$$

; where  $C = \mu_{\text{eff}}^2 / 8$  [11]

The effective magnetic moments per formula  $\mu_{\text{eff}}$  is about 5  $\mu_B$  for  $x=0.0$  and increases to about 7  $\mu_B$  for  $x=1.0$ . This increase of effective magnetic moments with  $x$  is due to the substitution of the magnetic  $\text{Pr}^{3+}$  ions. Moreover, we notice that with increasing magnetic  $\text{Pr}^{3+}$  concentration ( $x$ ), both  $\mu_{\text{eff}}$  and  $\mu_m$  are enhanced. In particular, they increase obviously around  $x=0.5-0.6$ . As well as  $\mu_{\text{eff}}$  and  $\mu_m$ , the  $x$ -dependences of  $T_C$  and  $T_G$  show an obvious increase around  $x=0.6$ . This may be interpreted as follows: the  $\text{Pr}^{3+}$  ions doping to La site induces the decrease of lattice constant and  $\text{Mn}^{2+}$ - $\text{Mo}^{5+}$  bond

length and in addition they have large 4f magnetic moments; consequently, the Pr substitution enhances the magnetic interaction. The present results indicate that the magnetic moments and critical temperatures obviously change around  $x=0.6$ , and the spin glass to cluster glass crossover also takes place at the same value of  $x$  at low temperatures.

In the present work, any sign of full magnetic ordering of 4f moments in  $\text{Pr}^{3+}$  was not observed down to 5 K. Although the 4f moments of rare-earth ions are expected to order magnetically at low temperatures, but because the  $\text{Pr}^{3+}$  ions occupy half of the A site of perovskite structure even in the  $x=1.0$  sample, therefore, the magnetic ordering of 4f moments of  $\text{Pr}^{3+}$  hardly occurs in this system. At low temperatures, however, the strong magnetic fluctuation of 4f moments may exist, and induce the ferromagnetic behavior of this system in higher Pr doping region, as shown in Fig. 6. The cluster glass may be also related with the fluctuation of 4f magnetic moments of  $\text{Pr}^{3+}$ .

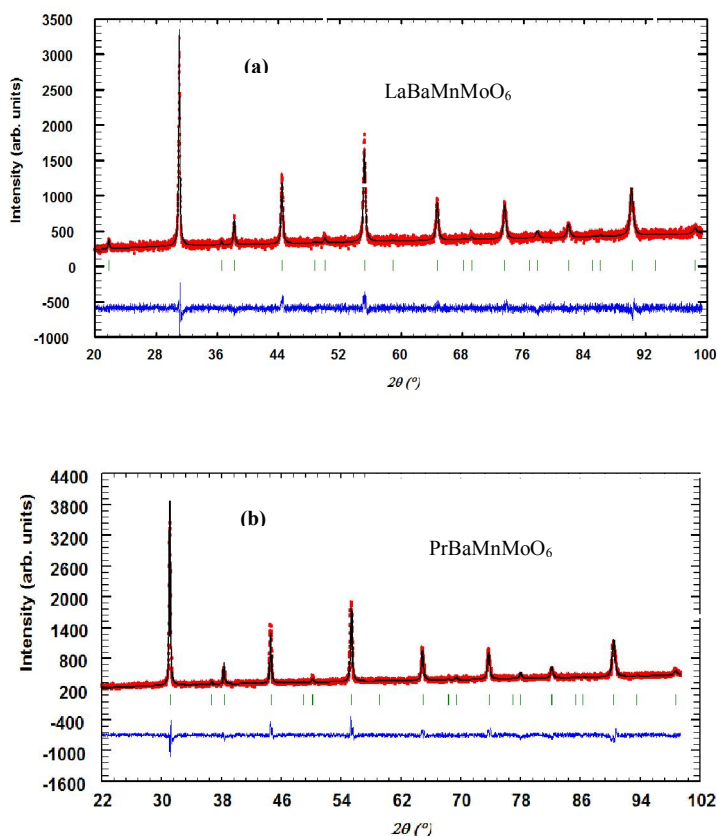
### 3.3 Resistivity Measurements

Figure 8(a) represents temperature-dependent resistivity for four samples of  $\text{La}_{1-x}\text{Pr}_x\text{BaMnMoO}_6$

with various Pr concentrations ( $x = 0.0, 0.2, 0.7$ , and  $1.0$ ). The temperature dependence of resistivity for all these samples exhibits a semiconducting behavior, that is, the resistivity decreases with increasing temperature. As shown in Fig. 8 (a), the absolute value of resistivity at 300K decreases almost two orders of magnitude upon Pr doping. This may be interpreted as a result of the decrease of  $\text{Mn}^{2+}\text{-Mo}^{5+}$  bond length, which enhances the hopping of carriers between the neighboring Mn/Mo sites. As shown in Fig. 8(b), the resistivity data can be well described by variable range hopping model equation (3) [8].

$$\rho = \rho_0 \exp(-T_0/T)^{1/4} \quad (3)$$

; where  $\rho_0$  and  $T_0$  are a temperature independent parameter and carrier localization parameter, respectively. The inset of Figure 8(b) shows the  $x$  dependence of  $T_0$ .  $T_0$  decreases, as the Pr concentration  $x$  is increased. This behavior also indicates that the carrier hopping increases due to the shrinkage of crystallographic lattice with Pr doping. In this system, however, the electronic structure seems to be essentially unchanged by the Pr substitution.



**Figure 1:** Typical powder x-ray diffraction profiles for  $\text{La}_{1-x}\text{Pr}_x\text{BaMnMoO}_6$  ((a)  $x=0$  and (b)  $1.0$ ). Dots and solid line represent the observed and calculated profiles, respectively. The difference plot is drawn below the profile, and vertical bars represent the allowed reflections.

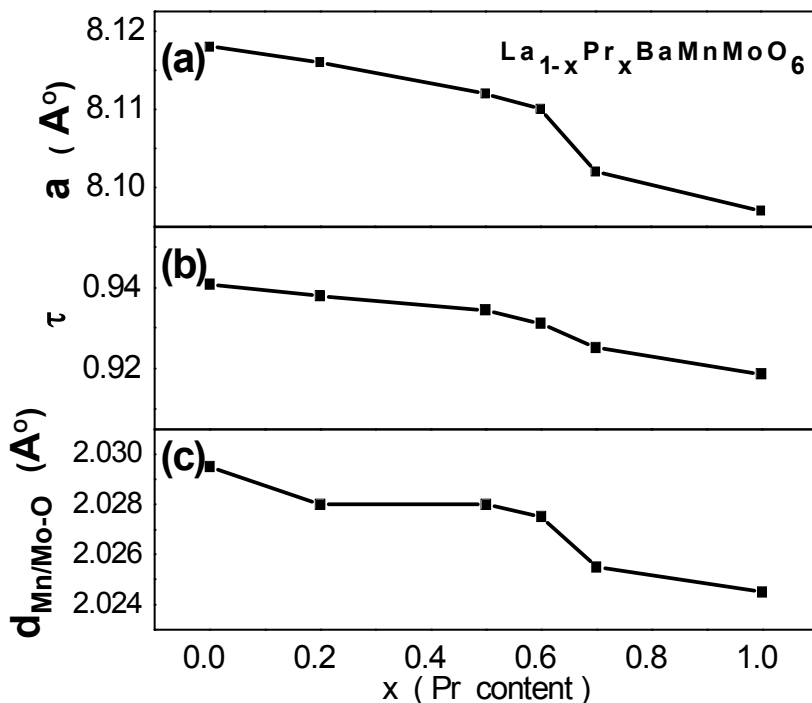


**Figure 2:** Pr concentration ( $x$ ) dependence of (a) lattice constant, (b) tolerance factor, and (c) bond length of  $d_{\text{Mn/Mo-O}}$  of  $\text{La}_{1-x}\text{Pr}_x\text{MnMoO}_6$ , respectively.

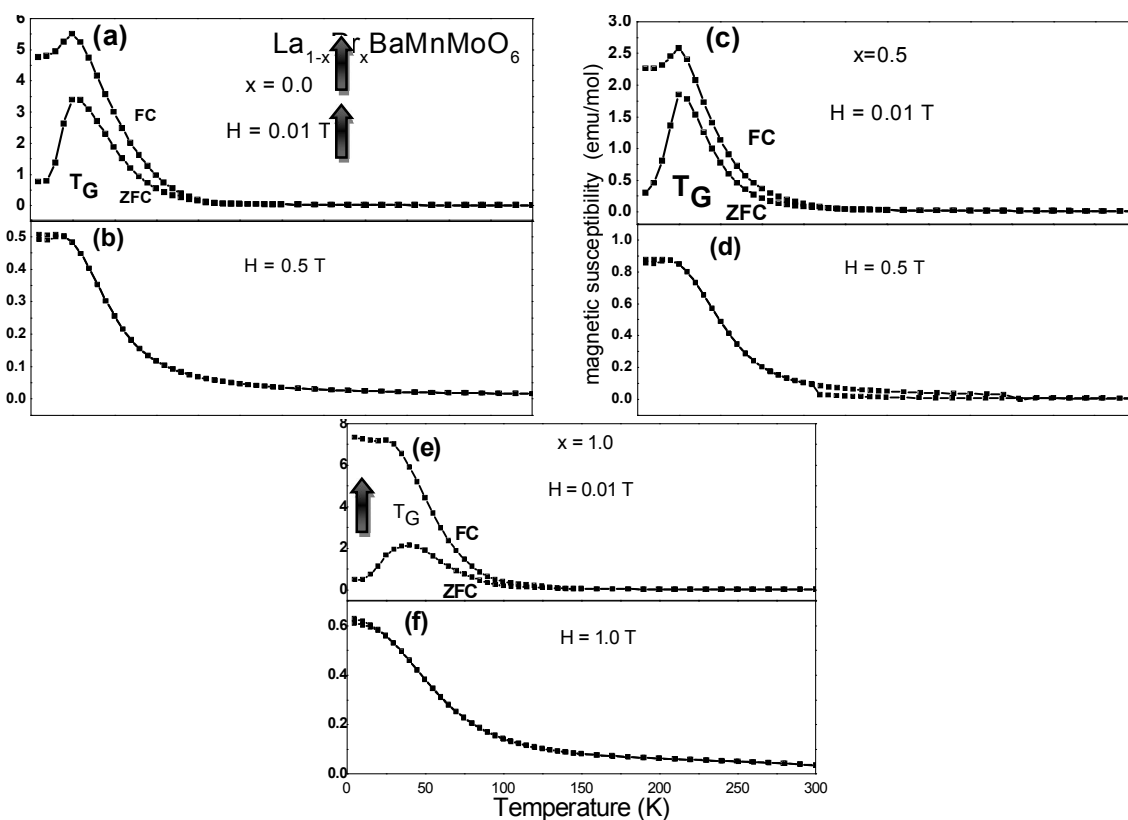
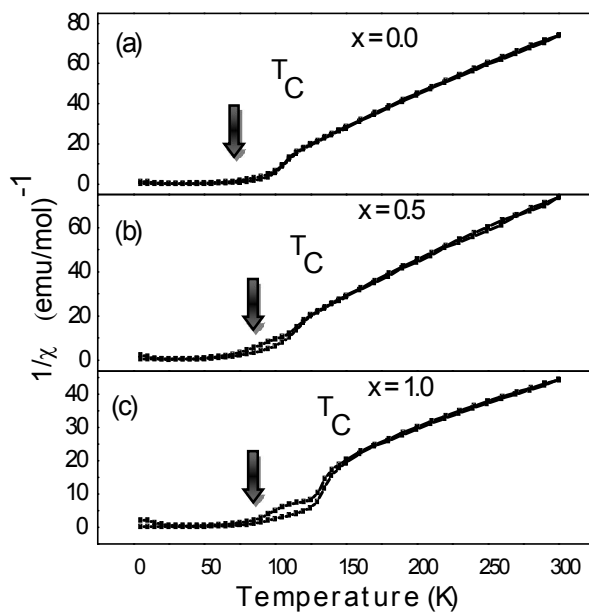
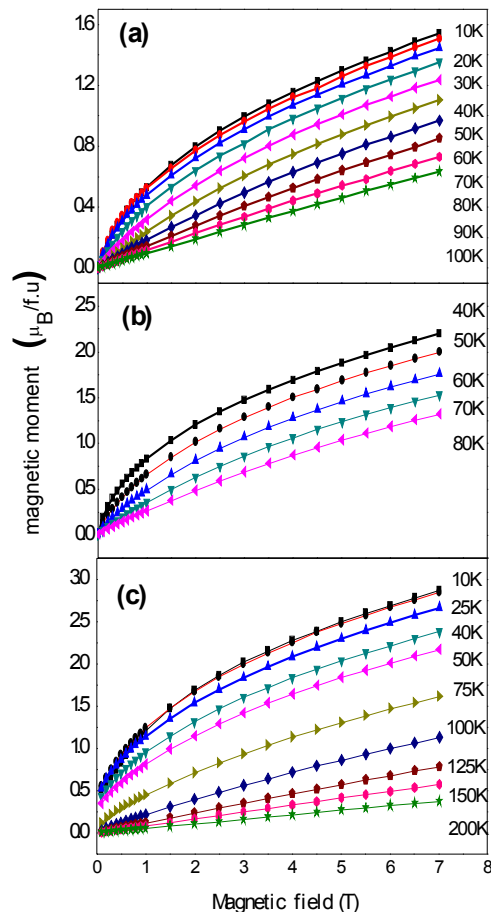


Figure 3: (a)-(f) Temperature dependence of magnetic susceptibility in various magnetic fields



**Figure 4:** (a)-(c) Inverse of magnetic susceptibility for  $\text{La}_{1-x}\text{Pr}_x\text{MnMoO}_6$  with  $x=0, 0.5$  and  $1.0$ , respectively.



**Figure 5:** (a)-(c) Magnetic field dependence of magnetic moment at various temperatures for  $\text{La}_{1-x}\text{Pr}_x\text{MnMoO}_6$  with (a)  $x=0$ , (b)  $0.5$  and (c)  $1.0$ , respectively.

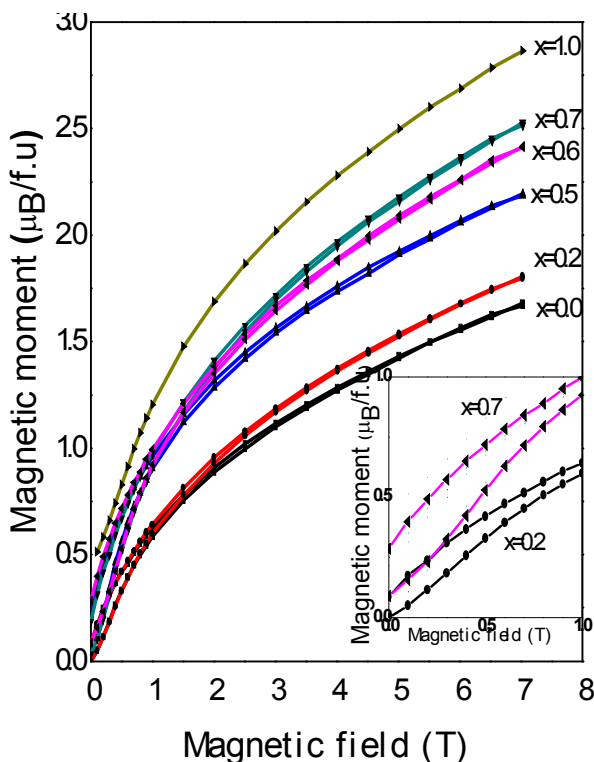


**Figure 6:** Magnetic field dependence of magnetic moment at 5 K for  $\text{La}_{1-x}\text{Pr}_x\text{MnMoO}_6$  with various Pr concentrations of  $x=0, 0.2, 0.5, 0.6, 0.7$  and  $1.0$ .

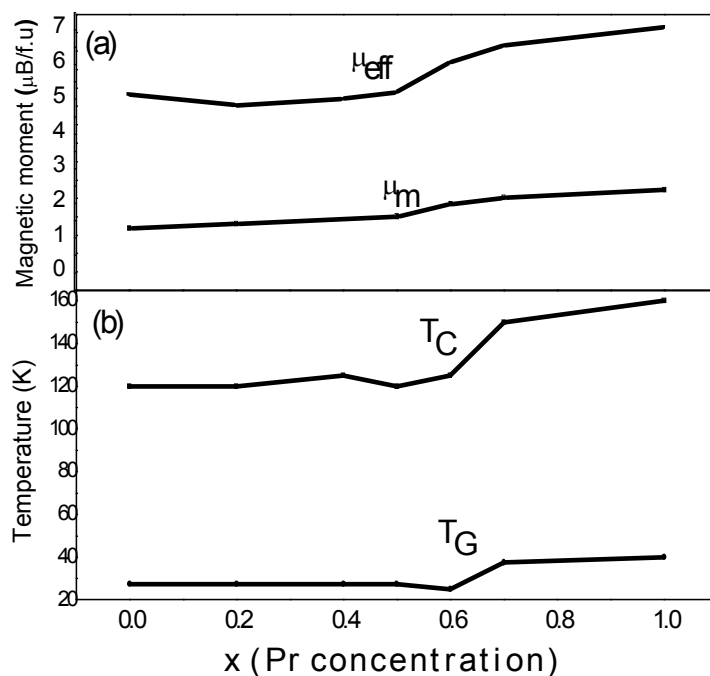


**Figure 7:** (a) Pr concentration ( $x$ ) dependence of magnetic moment ( $\mu_m$ ) at 5K in magnetic field of 7 T and effective magnetic moments ( $\mu_{\text{eff}}$ ) estimated by Curie-Weiss rule in paramagnetic region in  $\text{La}_{1-x}\text{Pr}_x\text{MnMoO}_6$ , respectively. (b)  $x$  dependence of magnetic transition temperatures,  $T_C$  and  $T_G$ , respectively.

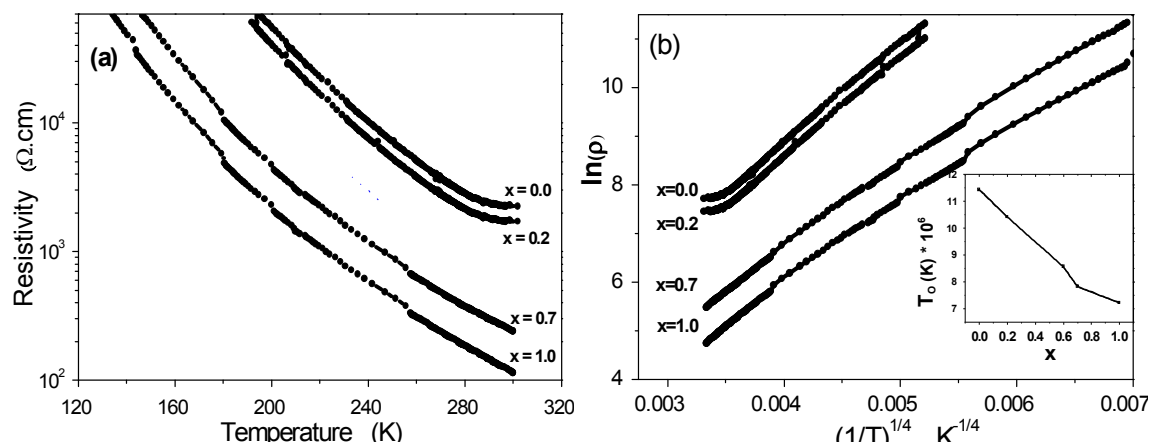


**Figure 8:** (a) Temperature dependence of resistivity for  $\text{La}_{1-x}\text{Pr}_x\text{BaMnMoO}_6$  with various Pr concentrations of  $x=0, 0.2, 0.7$  and  $1.0$ . (b) Resistivity vs.  $1/T^{1/4}$  plots for the samples with  $x=0, 0.2, 0.4, 0.7$  and  $1.0$ . Inset shows the  $x$ -dependence of electron localization parameter  $T_0$ , estimated by variable range hopping model.

## Conclusion

$\text{La}_{1-x}\text{Pr}_x\text{BaMnMoO}_6$  double perovskite system has been successfully prepared, and the structural, magnetic and electronic properties have been investigated. Polycrystalline  $\text{La}_{1-x}\text{Pr}_x\text{BaMnMoO}_6$  with  $x=0-1.0$  can be prepared under the condition of high sintering temperature and in the atmosphere of flowing of forming gas ( $\text{Ar}+\text{H}_2$ ) with high  $\text{H}_2$  concentration. The result of powder X-ray diffraction and the analysis indicate that the crystal structure of this system is cubic. The lattice parameter and the bond lengths of  $\text{La}/\text{Pr}/\text{Ba}-\text{O}$  and  $\text{Mn}/\text{Mo}-\text{O}$  decrease with Pr doping. The decrease of bond length enhances the magnetic interaction between nearest-neighbor Mn and Mo spins, and resultantly the ferrimagnetic transition temperature increases with Pr doping level. In the low Pr doping region, the low-temperature magnetic susceptibility shows spin glass behavior due to the competing between the nearest-neighbor and next-nearest-neighbor interactions. On the other hand, the highly doping of Pr enhances the magnetic interactions due to the shrinkage of crystal lattice. In addition, the results of magnetic susceptibility indicate that the Pr substitution enhances the ferromagnetic interaction and consequently induces the crossover from spin glass state to cluster glass one around  $x=0.6$  at low temperatures. In all the samples of  $\text{La}_{1-x}\text{Pr}_x\text{BaMnMoO}_6$ , the electric resistivity shows semiconducting behavior, and is described by the variable range hopping model. The decrease of bond lengths by Pr doping enhances the carrier hopping, and resultantly the magnitude of resistivity is suppressed.

## Acknowledgement:

This work was performed in Prof. S. Tajima lab, Physics Department in Osaka University, Japan.

## Corresponding author

**Meaz T.M**

Physics Department, Faculty of Science, Tanta University, 31527 Tanta, Egypt.

[tmeaz@yahoo.com](mailto:tmeaz@yahoo.com) & [tmeaz@science.tanta.edu.eg](mailto:tmeaz@science.tanta.edu.eg)

## References

- [1] Jha P., S. L. Samal, K. V. Ramanujachary, S. E. Lofland and A. K. Ganguli, (2005), Bull. Mater. Sci., 28, No. 6, 571-577.
- [2] Galasso F. S. (1969) Structure, Properties and Preparation of Perovskite type Compounds (Pergamon, London,).
- [3]. Patterson F. K, C. W. Moeller and R. Ward, (1963), Inorg. Chem. 2, 196-198.
- [4]. Kobayashi K. -I, T. Kimura, H. Sawada, K. Terakura and Y. Tokura, (1998) Nature 395, 677-680.
- [5]. Azad A. K, S. G. Eriksson, S. A. Ivanov, R. Mathieu, P. Svedlindh, J. Eriksson, H. Rundlof, (2004) J. Alloys and Comp. 364, 77-82.
- [6]. Munoz A, J. A. Alonso, M. T. Casais, M. J. Martinez-Lope and M. T. Fernandez-Diaz, (2002) J. Phys. :Condens. Matter. 14, 8817-8830.
- [7]. Martinez-Lope M. J, J. A. Alonso, M. T. Casais, (2003) Zeit. Natur. Sec. B, J. Chem. Sci. 58, 571-576.
- [8] Li S., M. Greenblatt, (2002) J. Alloys and Comp. 338 , 121-125.
- [9] Nakamura T., J. Choy, (1977) J. Solid State Chem., 20, 233-244.

- [10] Shizhe T., Z. Junchai, Q. Congde, J. Xiangling, J. Bingzheng, (2006) *J. Rare Earths* 24, 679-684.
- [11]. Lin Q, M. Greenblatt, E. N. Caspi, M. Avdeev, (2006) *J. Solid State Chem.* 179, 2086-2092.
- [12] Caspi E. N., J. D. Jorgensen, M. Lobanov, and M. Greenblatt, (2003) *Phys. Rev. B* 67, 13443 (11pp).
- [13] Horikubi T.and N. Kamegashira, (1999) *J. Alloys and Comp.* 287, 62-66.
- [14] Serrate D., J. M. De Teresa, and M. R. Ibarra, (2007) *J. Phys. : Condens. Matter.* 19, 023201 (86pp).
- [15]. Powell A. V, J. G. Gore and P. D. Battle, (1993) *J. Alloys and Comp.*, 201, 73-84.
- [16]. Karmakar S, S. Taran, B. K. Chaudhuri, H. Sakata, C. P. Sun, C. L. Huang, and H. D. Yang, (2006) *Phys. Rev. B*. 74, 104407 (10pp).
- [17] Klimczuk T., H. W. Zandbergen, Q. Huang, T. M. McQueen, F. Ronning, B. Kusz, J. D. Thompson and R. J. Cava, (2009) *J. Phys.: Condens. Matter* 21, 10580 (7pp).
- [18] Woo H., T. A. Tyson, M. Croft, and S. W. Cheong, (2004) *J. Phys.: Condens. Matter* 16, 2689-2705.
- [19] Wu J.and C. Leighton, (2003) *Phys. Rev. B* 67, 174408 (16pp).
- [20] Itoh M., I. Natori, S. Kuota, and K. Motoya, (1994) *J. Phys. Soc. Jpn.*, 63, 1486-1493.

6/8/6012